SUPPLEMENTAL MATERIAL

Hu et al., http://dx.doi.org/10.1084/jem.20160612

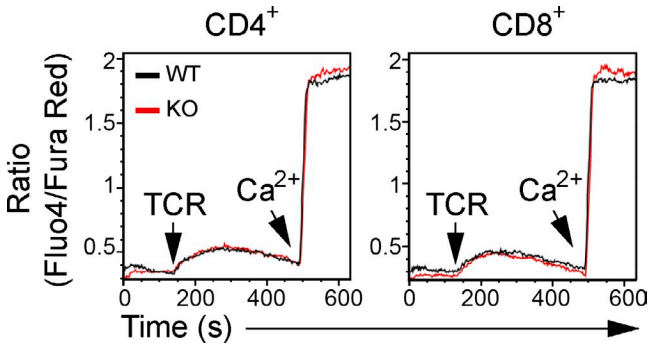

Figure S1. **TCR-induced calcium flux is independent of TMEM16F.** WT or TMEM16F-KO (KO) splenocytes were stained with Ca^{2+} indicator dyes Fura Red and Fluo-4 before stimulation by cross-linked anti-CD3 (5 µg/ml) at the indicated time (marked by arrows, TCR), followed by CaCl2 (marked by arrows, Ca^{2+}). Intracellular Ca^{2+} amounts are shown as a median ratio of Fluo-4/Fura Red over time.

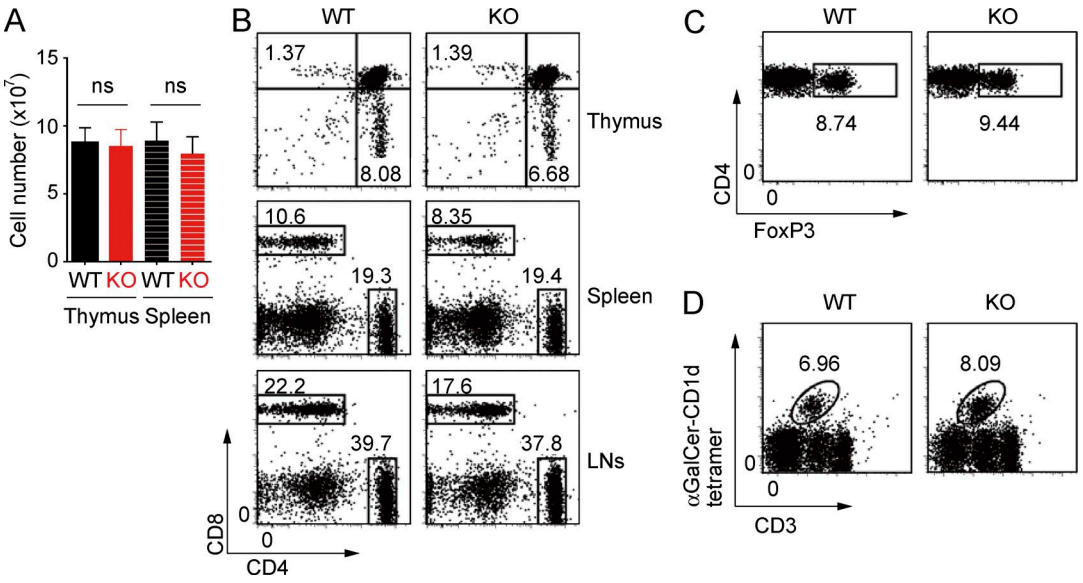

Figure S2. **Normal T cell development in TMEM16F-KO mice.** (A) Total lymphocyte numbers of thymus and spleen from WT or TMEM16F-KO mice. Results are displayed as mean ± SEM. (B–D) Frequencies of conventional T cells in thymus, spleen, and lymph nodes (LNs; B), T reg cells in spleen (C), and liver invariant NKT cells (D) assessed by flow cytometry. Data are representative of two to four independent experiments (n = 4–5 mice per group). Student's t test was used. ns, not significant.

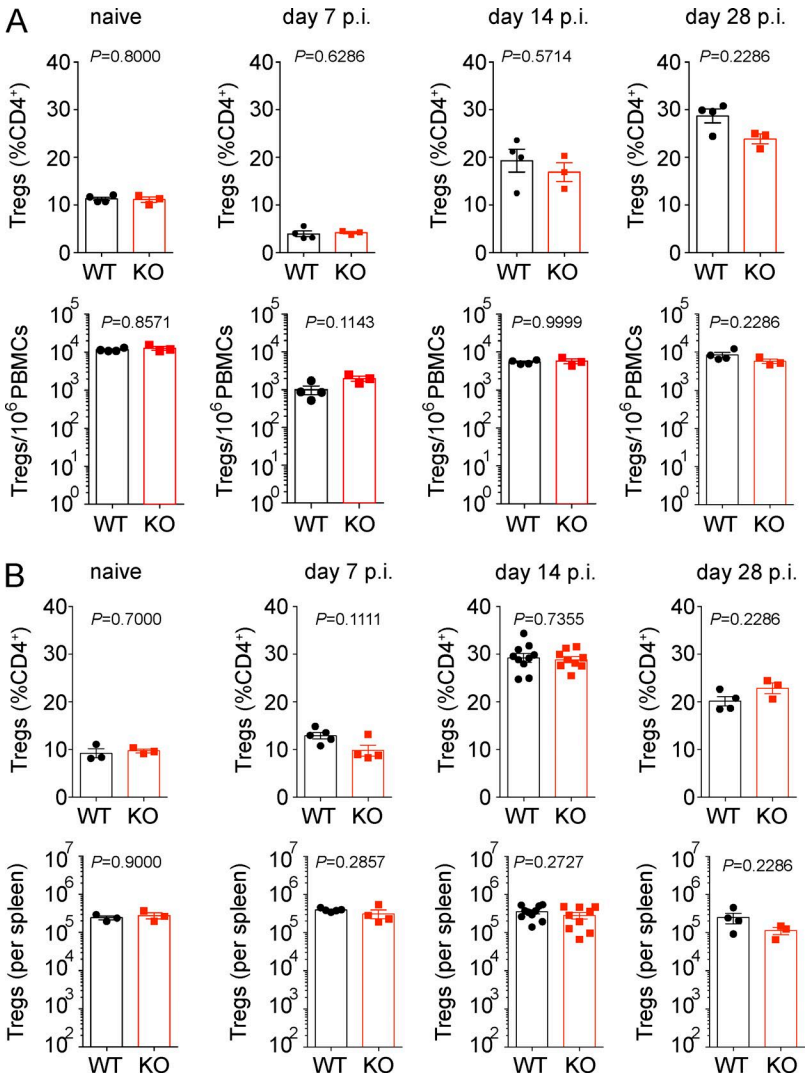

Figure S3. **T reg cell population in TMEM16F-KO and control mice during LCMV-C13 infection.** Flow cytometry analysis of T reg cells (FoxP3$^+$) in PBMCs (A) or splenocytes (B) from TMEM16F-KO or WT mice at indicated time points after LCMV-C13 infection. Frequencies (A and B, top row) and absolute cell number (A and B, bottom row) of T reg cells are shown. Data are representative of two to four independent experiments (n = 3–10 mice per group). Mann–Whitney U test was used.

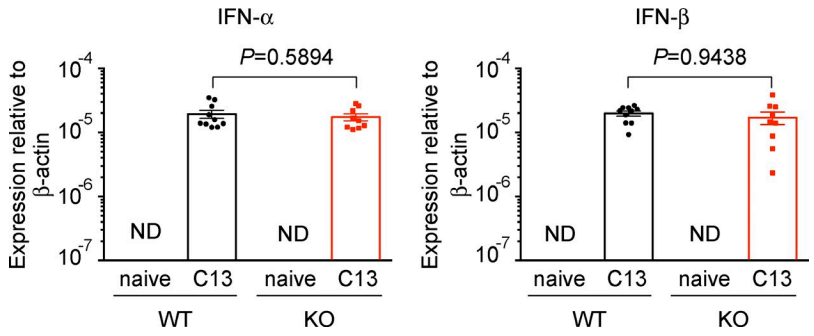

Figure S4. **Expression of type I IFN in TMEM16F-KO and control mice during LCMV-C13 infection.** mRNA level of IFN-α (left) and IFN-β (right) in spleen from LCMV-C13–infected mice (day 14 after infection) was determined by real-time PCR. Relative expression of IFN-α (left) or IFN-β (right) to β-actin was plotted. CT (threshold cycle) for IFN-α and IFN-β was measured between 28 and 31. *n* = 10 for WT and *n* = 9 for KO. No signal was detected in samples from naive mice after 40 cycles of amplification. ND, not detectable. P-value was determined by Mann–Whitney *U* test.

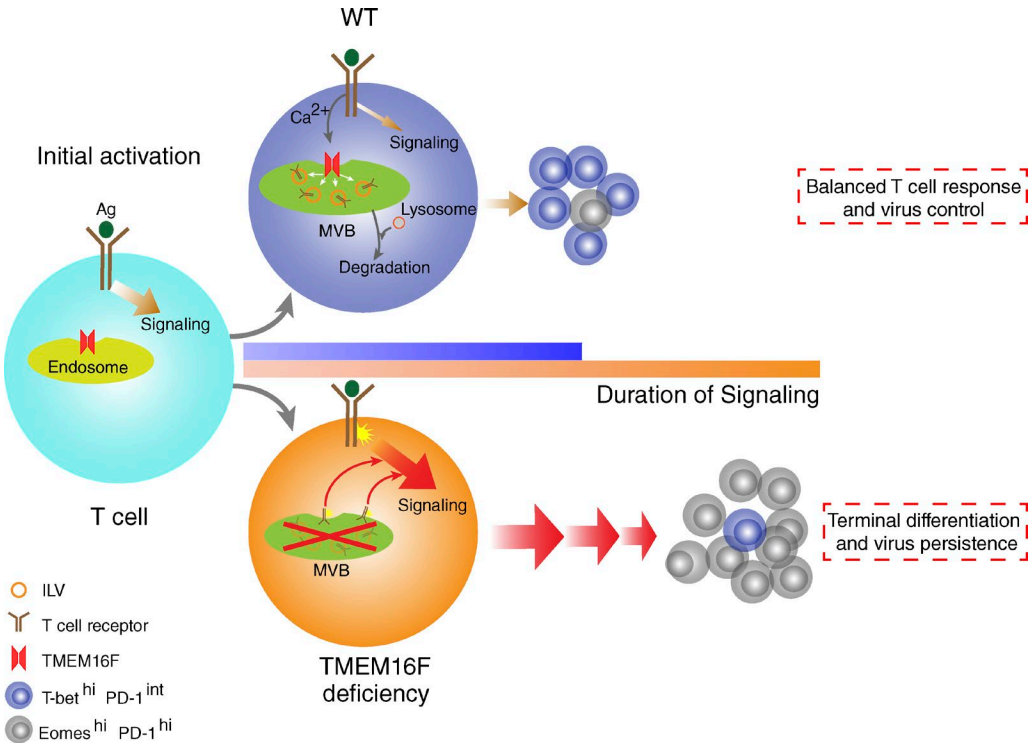

Figure S5. **Mechanistic model.** (top) TCR engagement, via increased intracellular Ca^{2+} levels, activates scramblase TMEM16F in late endosomes to mediate the formation of MVBs. Newly generated MVBs sequester intracellular TCR signaling complexes for subsequent lysosomal degradation to terminate T cell activation. This TMEM16F-mediated checkpoint determines the duration of signaling and the proper ratio of T-bet^{hi} to Eomes^{hi} effector T cells to facilitate virus clearance. (bottom) In the absence of TMEM16F, generation of MVBs is hampered, TCR signaling molecules accumulate, and T cell activation is sustained. Breaking the TMEM16F checkpoint leads to prolonged signaling that shifts the balance toward terminally differentiated Eomes^{hi} T cells and ultimate loss of virus protection.

Video 1. **Dynamic recruitment of TMEM16F to the IS.** Live imaging of Jurkat cells expressing TMEM16F-RFP by TIRF microscopy shows the dynamic recruitment of TMEM16F to the IS upon antigen stimulation. Cells were stimulated on 10 µg/ml αCD3-coated coverslips. Images were taken at the rate of one frame per 2 s for 348 s. Red, TMEM16F.

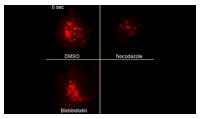

Video 2. **Disruption of microtubules, but not actin–myosin contractions, blocks the recruitment of TMEM16F to the IS.** TIRF live imaging of Jurkat cells pretreated with vehicle (DMSO, top left), 1 µM nocodazole (top right), or 1 µM blebbistatin (bottom left) before stimulation on 10 µg/ml αCD3-coated coverslips demonstrates that movement of TMEM16F-RFP toward the IS depends on microtubules but not actin. Images were taken at the rate of one frame per 0.5 s for 149 s. Red, TMEM16F.

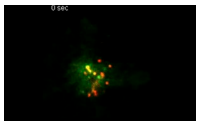

Video 3. **TMEM16F mainly resides in a Rab7-positive late endosomal compartment.** Dynamic movements of TMEM16F and Rab7 at the IS reveal that TMEM16F mainly resides in a Rab7-positive late endosomal compartment. TIRF live images of Jurkat cells overexpressing TMEM16F-RFP and Rab7-GFP placed on 10 µg/ml αCD3-coated coverslips were taken at the rate of one frame per 0.5 s for 150 s. Pearson's coefficient, 0.727. Red, TMEM16F; green, Rab7.

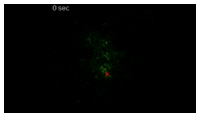

Video 4. **TMEM16F is not localized in Rab5-positive early endosomes.** Dynamic movements of TMEM16F and Rab5 at the IS reveal that TMEM16F is not spatially correlated with Rab5. TIRF live images of Jurkat cells overexpressing TMEM16F-RFP and Rab5-GFP placed on 10 µg/ml αCD3-coated coverslips were taken at the rate of one frame per 0.5 s for 150 s. Pearson's coefficient, 0.186. Red, TMEM16F; green, Rab5.

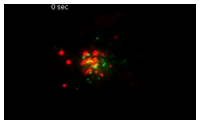

Video 5. **TMEM16F is not localized in Rab11-positive recycling endosomes.** Dynamic movements of TMEM16F and Rab11 at the IS reveal that TMEM16F is not spatially correlated with Rab11. TIRF live images of Jurkat cells overexpressing TMEM16F-RFP and Rab11-GFP placed on 10 µg/ml αCD3-coated coverslips were taken at the rate of one frame per 0.5 s for 149 s. Pearson's coefficient, 0.217. Red, TMEM16F; green, Rab11.

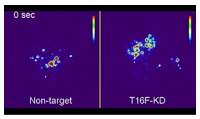

Video 6. **Sustained TCR phosphorylation in the absence of TMEM16F.** Tracking of phosphorylated TCRs using a live-cell reporter (mCherry-tSH2 (ZAP70)) demonstrates that phosphorylation of TCR is sustained in the absence of TMEM16F (T16F-KD) when compared with control (nontarget). Jurkat cells overexpressing mCherry-tSH2 (ZAP70) were stimulated on 10 µg/ml αCD3-coated coverslips. Images were taken by TIRF microscopy at the rate of one frame per 2 s for 300 s. Heat map of mCherry-tSH2 intensity is shown. Red, mCherry-tSH2.

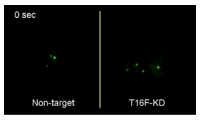

Video 7. **Enhanced and sustained formation of LAT microclusters shows hyperactivation of T cells when TMEM16F is lacking.** Dynamics of LAT microclusters in activated Jurkat cells were monitored by TIRF microscopy. Jurkat cells overexpressing LAT-YFP were stimulated on 10 µg/ml αCD3-coated coverslips. Images were taken by TIRF microscopy at the rate of one frame per 5 s for 360 s. Green, LAT.